Journal of Thermal Analysis, Vol. 50 (1997) 727-744

MODULATED DIFFERENTIAL SCANNING CALORIMETRY
The effect of experimental variables

F. Cser, F. Rasoul and E. Kosior

CRC for Polymers Pty. Ltd., 32 Business Park Drive, Notting Hill, VIC 3168
and Polymer Technology Centre, Royal Melbourne Institute of Technology, Melbourne VIC 3000, Australia

(Received November 29, 1996)

Abstract

The reproducibility and reliability of the TA Instruments Modulated Differential Scanning Calorimeter (MDSC) was tested over a range of conditions. The equipment base line was found to be fairly constant with a very small fluctuation (10 μW), which means a 0.1% fluctuation on the scale of a normal polymer MDSC curve. The excellent stability of the base line and the reasonable reproducibility of the curves (5%) suggest that frequent calibration is not required.

The heat capacities calculated from the modulated response to the variable temperature depend on the frequency for a given cell constant. The heat capacity cell constant is a unique function of the modulation frequency:

$$K_c = K_c^0 \, p/(p-6.3)$$

where p is the time of the periodicity expressed in seconds and K_c^0 is the heat capacity cell constant measured on a standard material and reduced to zero frequency. The cell constants depend on the flow rate of the helium according to:

$$K(He) = K^0(1.298-0.004424He+1.438\cdot10^{-5}He^2)$$

where He is the flow rate of helium in ml min^{-1} and K^0 represents a constant at 100 cm^3 min^{-1}. There is a strong dependence of cell constant on the flow rate ranges from 10 to 80 cm^3 min^{-1}, while above this rate (up to 135 ml min^{-1}) the cell constant approaches a plateau.

Keywords: frequency dependence, heat capacity, MDSC, thermal analyses

Introduction

Basics of MDSC

Modulated DSC (MDSC) was developed by Reading *et al.* [1, 2] and was produced commercially by TA Instrument. It combines a linear change of tempera-

0368–4466/97/ $ 5.00

John Wiley & Sons Limited
Chichester

ture with a sinusoidal modulation in a heat flow type of DSC cell. This enables the instrument to record the heat capacity of the sample parallel with the heat flow, because of the modulated change of the temperature. The response function (instantaneous heat flow) of the tested material to the temperature function is compared for normal and modulated measurements in Table 1 [3–5]:

The total heat flow can be divided into two parts, i.e. the reversible and kinetic heat flows according to Eq. (1):

$$\left(\frac{dQ}{dt}\right)_{total} = \left(\frac{dQ}{dt}\right)_{reversibile} + \left(\frac{dQ}{dt}\right)_{kinetic} \quad (1)$$

where the reversible heat flow is defined by Eq. (2):

$$\left(\frac{dQ}{dt}\right)_{reversibile} = -C_p(T)\beta \quad (2)$$

i.e. the heat capacity multiplied by the negative of the overall rate of temperature change (β see Table 1).

The equipment records the actual (modulated) temperature, the instantaneous (modulated) heat flow in response to temperature function and phase angle of these two harmonic functions. If the change in the temperature is within the harmonic range (which depends on the parameters of the modulation, the actual temperature, the overall heating rate and the power of the heating/cooling devices) a Fourier analysis of the response of the temperature function will result in two functions: the heat capacity (C_p) which is determined mainly by the amplitude of the responses, and the total heat flow which is the average of the heat flow, ΔH_t. The Fourier analysis uses one and a half periods of the modulation and it will produce an artificial peak if there are less than 4 modulation periods through a transition [3–5].

The problem

Several publications have appeared in the literature in the recent years dealing with the theoretical background of the MDSC, particularly with the steady state conditions of the modulated or oscillating DSC cell [6–8]. In this paper we present our experiences with the TA MDSC Instrument and to show its reproducibility. The influence of various equipment parameters on the measured caloric data are also presented. These parameters are cell constants, rate of heating/cooling, modulation frequency, and rate and quality of the purging gas.

The cell constant is determined by the geometry and the construction of the cell, and is given by the producer upon delivery of the equipment (primary calibration). In this study it has been recalibrated by new sets of calibrating parameters, using indium as the standard material, with different heating rates.

Table 1 The basic functions of normal and modulated DSC

DSC	MDSC
Temperature change	
$T(t)=T_0+\beta t$	$T(t)=T_0+\beta t+A_T\sin(\omega t)$
$T(t)$=program temperature [K]	A_T=amplitude of temperature modulation [±C°]
T_0=starting temperature [K]	$\omega=2\pi/p$ the modulation frequency [s^{-1}]
β=linear heating rate [K min^{-1}]	p=period [s]
t=time [min]	
Instantaneous heat flow	
$dQ/dt=C_p(\beta)+f(t,T)$	$dQ/dt=C_p(\beta+A_T\omega\cos(\omega t))+f'(t,T)+A_K\sin(\omega t)$
dQ/dt=total heat flow [W g^{-1}]	$(\beta+A_T\omega\cos(\omega t))$=measured heating rate [$dT/dt$]
C_p=heat capacity [Joule $g^{-1}K^{-1}$]	$f'(t,T)$=kinetic response without modulation [W g^{-1}]
T=absolute temperature [K]	A_K=amplitude of kinetic response to temperature modulation
$C_p(\beta)$=heat capacity component [W g^{-1}]	
$f(t,T)$=kinetic component [W g^{-1}]	

According to the basic equations of MDSC, the apparent heat capacity is a function of the modulation frequency (Eq. (36) in Ref. [5]) and has the form shown in Eq. (3):

$$K_c = B\sqrt{1 + \left(\frac{C'\omega}{K}\right)^2} \tag{3}$$

where K_c is the heat capacity cell constant, B is a scaling factor, C' is the heat capacity of the reference pan and K is the cell constant.

A series of experiments using the same sample and sample position was conducted to study the influence of the modulation frequency on the total heat flow and the heat capacity. The results showed that the heat capacity and hence the K_c value, do not show the dependence on the modulation frequency indicated by Eq. (3). It has also been observed that the quality and flow rate of the purging gas influence the numeric value of the cell constant as well as the observed heat capacities. In this paper we investigate the magnitude of these effects and also ways to carry out the necessary corrections if the actual parameters are different from those used in the calibration.

Experimental

Equipment and experimental conditions

TA Instruments MDSC 2920 with the Thermal Analyst 2100 computing system was used. The parameters have been varied within the limitations determined by the hardware and given in the equipment manual [3]. For the calibra-

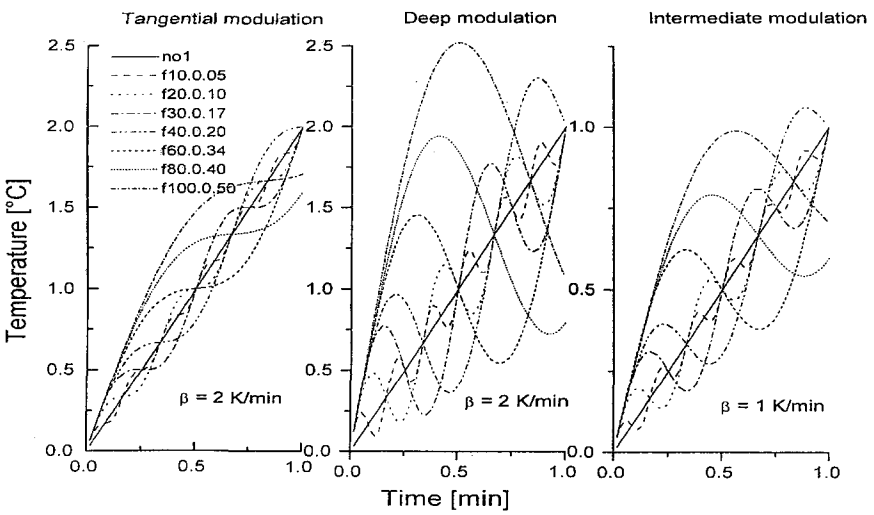

Fig. 1 Temperature functions used in the studies on the dependence of the heat capacities on the modulation frequency

tion of the equipment, indium and sapphire (with a mass of 60.59 mg and supplied by the TA) were used. Heat capacities of different polymers have also been measured at different frequencies. From the basic recorded data only representative results will be shown here to prove the reliability of the equipment, and the capability of the data analysis method and the software, which is supplied by TA Instruments.

The overall heating/cooling rate (β) was varied from 0.1 to 5 K min^{-1} in the base line and melting heat calibration experiments.

Heat capacity measurements were carried out with β=2 K min^{-1} heating and cooling rates. The resolution and the optimal noise to signal ratio depend on the maximum heating/cooling rate. Low modulation amplitude values (depending on the modulation frequency) were selected to achieve "zero heating during the cooling event" or "zero cooling during the heating event". This was called tangential modulation (left hand part of Fig. 1). The heating/cooling capacity of the equipment, together with the geometry and heat capacity of the measuring cell, determine a maximal depth of modulation without affecting the harmonic character of the temperature fluctuation. This was approached by a so-called deep modulation (middle part on Fig. 1) as another extreme example. When the amplitude was 3 times the amplitude used for the tangential modulation, the limits of the hardware were not approached. Reliable results could be obtained also with intermediate or medium modulation (right hand part on Fig. 1), where a small cooling during heating was allowed.

Helium was used as the purging gas and a fairly constant (100 ml min^{-1}) flow rate was maintained during the entire evaluation experiments. Some of the heat capacity experiments have been repeated using different flow rates of helium (0 to 130 ml min^{-1}) to show the effect of this parameter on the data. Nitrogen was also tried as a purge gas but it was later abandoned because results obtained from helium purging showed smoother (less noisy) DSC curves.

Methods of calculation

The dependence of the heat capacities on the modulation period was approximated by reading the measured heat capacities values of the samples at definite temperatures and the values were represented as a function of the reciprocal of the modulation period (modulation frequency). The functions have been extrapolated to zero frequency (heat capacities reduced to zero frequency) and the measured heat capacities have been divided by these reduced values, which are characteristic for each temperature. A universal function has been obtained using this method and the mean value of the slopes have been calculated by a least square fit of the data (first, second or third order fits were calculated).

With the new form of the frequency dependence of the heat capacities, the curves have been normalised by their hypothetical zero frequency value so that they could be compared with each other in order to obtain their estimated stand-

ard error due to transformation. The transformed forms of the curves have been checked by other experiments in three different tests where the new heat capacity constant was used to obtain the real MDSC curve.

The reproducibility of the curves have been calculated in the following way:

1. The data are recalculated to the same temperature using an interpolation of the measured values (integer scale of temperatures).

2. The mean value of the total heat flow and the heat capacities, as will be shown later, have been calculated commencing with the measured values from the individual runs at each temperature.

3. The error (E_1) arising from the actual mean values was calculated from Eq. (4), while the difference of the mean values (E_2) related to the curves was calculated from Eq. (5)

$$E_1 = \frac{1}{T_e - T_o + 1} \sum_{T=T_o}^{T_e} \left(\frac{\sqrt{\frac{1}{nfr} \sum_{i=1}^{nfr} (\nu(i,T) - \langle \nu(T) \rangle)^2}}{[\nu(T)]} \right) \quad \text{where} \quad \langle \nu(T) \rangle = \frac{1}{nfr} \sum_{i=1}^{nfr} \nu(i,T) \tag{4}$$

$$E_2 = \frac{\sum_{T=T_o}^{T_e} \sqrt{\frac{1}{nfr} \sum_{i=1}^{nfr} (\nu(i,T) - \langle \nu(T) \rangle)^2}}{\sum_{T=T_o}^{T_e} \langle \nu(T) \rangle} \tag{5}$$

where T_o and T_e are the initial and final temperatures for the integrated area; *nfr* is the number of curves at different frequencies used for the calculation, $\nu(i,T)$ is either the total heat flow or heat capacity of temperature t recorded by the i^{th} frequency run. At least 30 data points were used in the error calculations; however, in some cases the whole temperature range could be used (120–160 data points).

Statistically the error distribution $E_1 \approx E_2$. However, if there was a systematic error ($E_2 >> E_1$).

Materials

High purity indium, supplied by TA, is the enthalpy standard used, it has the following value: T_m=156.28°C and ΔH_m=28.42 J g^{-1}. Sapphire, also supplied by TA, was used as the heat capacity (C_p) standard. HDPE (HDS148), Kemcor product, is an extrusion grade high density polyethylene (MFI value 0.9–2.0). Polypropylene (GWM22), ICI Australia product, is an injection moulding grade (MFI=4). LDPE (WNC176), ICI Australia product, is a film blowing grade low density polyethylene (MFI=0.4). Kodapak-PET 9921W, Eastman Chemical product, is a bottle grade copolymer (Mn=25000 g mol^{-1}).

The samples were accurately weighed and encapsulated in the supplied (TA) pans covered by the proper lids. An empty pan with lid was used as a reference. Pans supplied by TA were found to have the same weights within ±0.1 mg, and therefore matching their weights with the reference pan was not necessary [3].

Both PET samples were virgin, i.e. freshly cut from injection moulded bars prior to the test (3.61 and 17.04 mg). This procedure was followed to show the effect of modulation periodicity on the cold crystallisation between 110 and 125°C. The heating/cooling cycle of these samples was immediately repeated to eliminate cold crystallisation, which is due to the slow cooling rates during the first cycle. All the data generated from the second run at various heating/cooling rates were compared in order to extrapolate the data to zero frequency and recalculate the mean error at this frequency.

All other polymers were exposed to a heating and cooling cycle at 2 K min^{-1} rates, before MDSC measurements to eliminate their thermal history. Sample weight of 8–12 mg were used for the different modulation periods.

Results and discussion

Baseline

The baseline was checked with an empty cell, at various heating rates. A zero modulation amplitude was applied and the total heat flow was recorded using a 90–100 ml min^{-1} flow rate of helium. The recorded baselines between 20 and 150°C at various heating/cooling rates (from 0.1 to 5 K min^{-1}) are shown in Fig. 2.

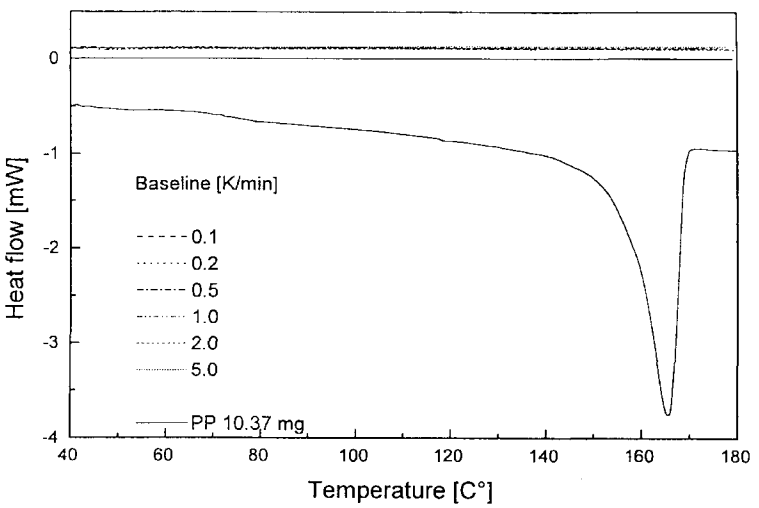

Fig. 2 The recorded base lines in a comparison with a real recording using 10.37 mg of polypropylene

The overall average variation of the baseline is less than 10 μW at each heating rate and this is in the order of 0.1% of the peak maximum obtained in a normal run for a semi crystalline polymer (e.g. see polypropylene, PP in Fig. 2) with a sample weight above 5 mg. It is also worth noting that the time required for the run at 0.1 K min^{-1} rate is more than 14 h.

Calibration for the heat flow and the temperature

Figure 3 shows the melting curves of indium. The measured signal for the heat flow is proportional with the heating rate (β) therefore the heat flow values shown in Fig. 3 have been recalculated as they would have been measured at a 2 K min^{-1} heating rate for comparison purposes. The melting enthalpy values and the peak temperatures are presented as a function of heating rates in Table 2. The experiments were carried out using a 90–100 ml min^{-1} flow rate of helium. The calibration by TA Instruments, when originally installed, was conducted using 20–30 ml min^{-1} flow rate.

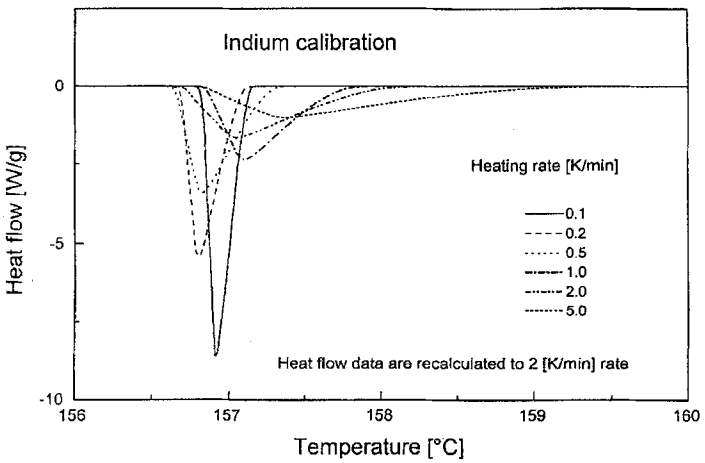

Fig. 3 Calibration of the cell constant by indium with different heating rates

A 0.1 K min^{-1} heating rate resulted in a 5% greater melting enthalpy than the mean value of the other runs at higher heating rates. The variation of the melting enthalpy with rates above 0.1 K min^{-1} is 0.541 J g^{-1}, i.e. a 1.62% deviation from the mean value. There are two different temperature values where the onset of the melting peaks are grouped: 156.65 and 156.82°C respectively.

The peak of the indium melting enthalpy is significantly broader with increased heating rate. This indicates a longer time constant for the heat flow, which is related to the heating rate limitation of the TA Instrument MDSC (5 K min^{-1}).

The theoretical values of the melting enthalpy and temperature for indium are 28.42 J g^{-1} and 156.83°C respectively. The mean melting enthalpy value for the all rates, with exception of 0.1 K min^{-1}, was 4.9 J g^{-1} above the theoretical value. The calibration has been repeated at the β=2 K min^{-1} heating rate using the standard cell constant and the melting enthalpy of indium was found to be 28.40 J g^{-1}.

Calibration for the heat capacity at different frequencies

Calibration was carried out at the β=2 K min^{-1} heating/cooling rate using modulation periods (p) of 10, 15, 20, 30, 40, 60, 80 and 100 s. The amplitude of modulation was selected to be proportional to the time of periodicity in order to keep the maximal and minimal heating/cooling rate constant (Fig. 1). In tangential modulation the amplitude was calculated from $(A_T)^t=160/p$ with p in seconds, while for deep modulation, the $(A_T)^d=3(A_T)^t$ relationship was used. These series of experiments were then repeated by using β=1 K min^{-1} for HDPE with a medium depth modulation where $(A_T)^m=2(A_T)^t$ was applied.

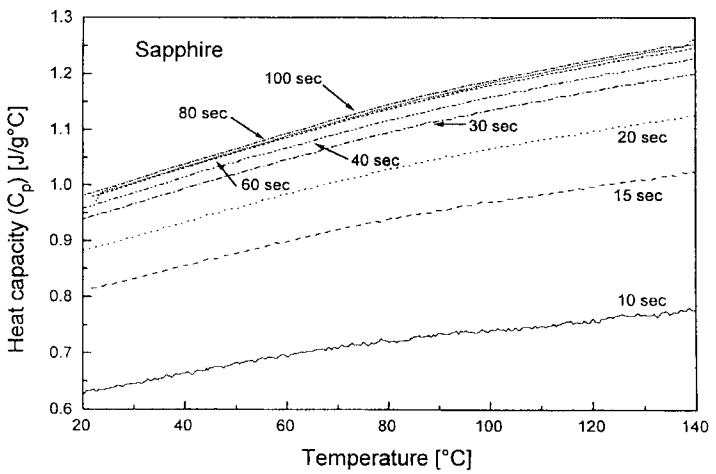

Fig. 4 Heat capacities of the sapphire at different modulation frequency using deep modulation

Sapphire

Figure 4 shows the heat capacity *vs.* temperature of sapphire measured at different modulation periodicity. Figure 5 represents the heat capacities at different temperatures of sapphire plotted as a function of the modulation frequency. It can be seen clearly that there is a second order decrease in the heat capacities. Eq. (6) is considered to be the best fit of the data:

$$C_p^o(T) = A_p^p(T)K_{C_p}p^2/(p^2-0.84p-29.22) \quad (6)$$

where C_p^o is the zero frequency heat capacity and A_p^p is the amplitude measured by p modulation period and K_{C_p} is the heat capacity cell constant. Its value is 0.8919 in our case. It has been calculated using the following heat capacity values for the sapphire: 0.9429, 0.8720 and 0.7792 J (g K)$^{-1}$ for 400, 350 and 300 K respectively [10].

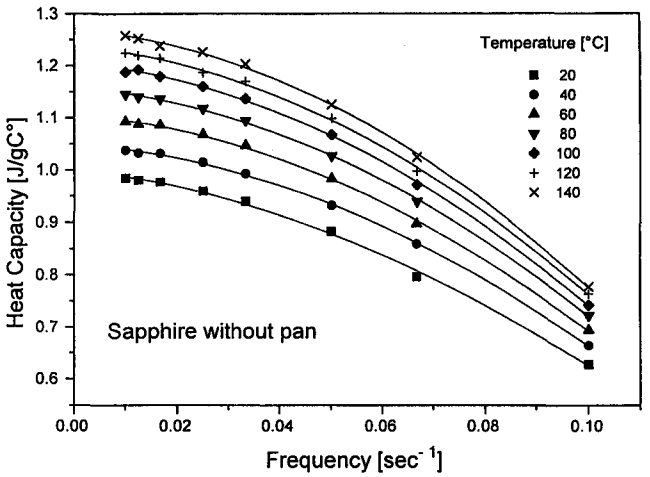

Fig. 5 The dependence of the heat capacities of sapphire on the modulation frequency

Polymers

The heat capacities of HDPE measured at different modulation frequencies with a tangential modulation amplitude are represented in Fig. 6. A strong frequency dependence is evident and explicitly shown in Fig. 7. The heat capacities show an almost linear reduction with increasing frequencies. This data is well fitted by Eq. (7) which is equivalent to:

$$C_p(0) = C_p\left(\frac{1}{p}\right)p/(p-K) \quad (7)$$

where the value of the constant (K) is 6.22±0.061 s.

The above Eq. differs from that given by the ATHAS group (Eq. (3)). The decrease of heat capacities with frequency given by TA Instruments in their user manual as well as by Wunderlich [3, 4] is much greater than that measured at our laboratory using a TA Instruments MDSC. The constants given by Wunderlich [4] did not accurately fit the present heat capacity data. (The condition used for the measurement of the heat capacity constants are not given in the Wunderlich report).

Figure 8 shows the total heat flow of HDPE measured at different modulation frequencies and tangential modulation amplitude. The different DSC curves are nearly indistinguishable at most temperatures, however, there are major differences at the melting and the crystallisation region. Because the crystallisation is a very fast process and it is usually completed within 1–2 min, larger heat capacity peaks are observed if smaller frequencies during cooling are used (p=60–100 s on Fig. 6). This anomalous behaviour may be an artefact caused by the Fourier transformation.

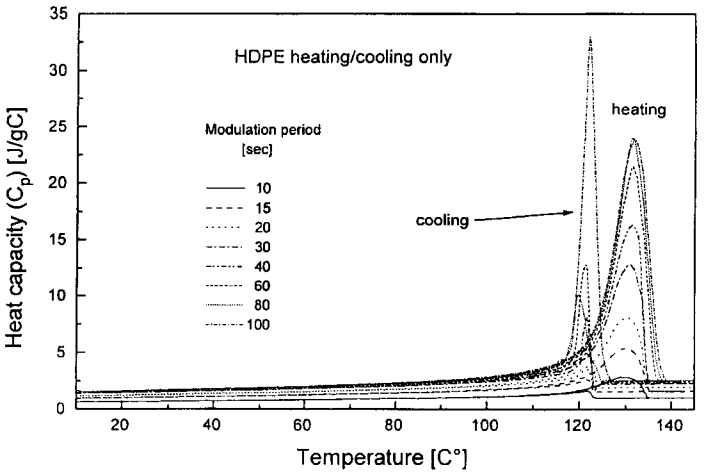

Fig. 6 The heat capacities of the HDPE recorded with different modulation frequencies and with tangential modulation amplitudes

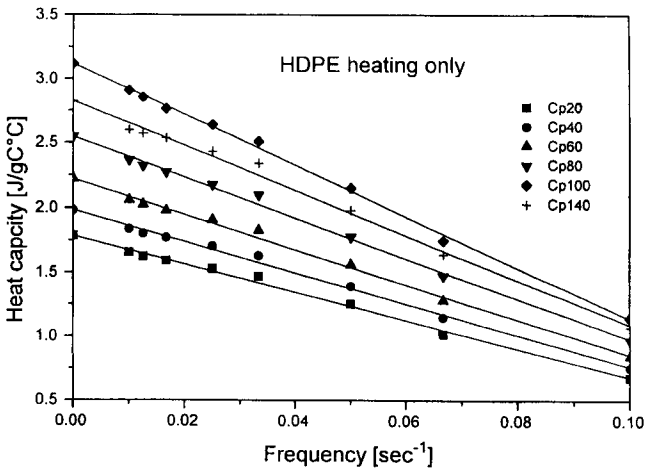

Fig. 7 The dependence of the heat capacities of HDPE on the modulation frequency using tangential modulation amplitude

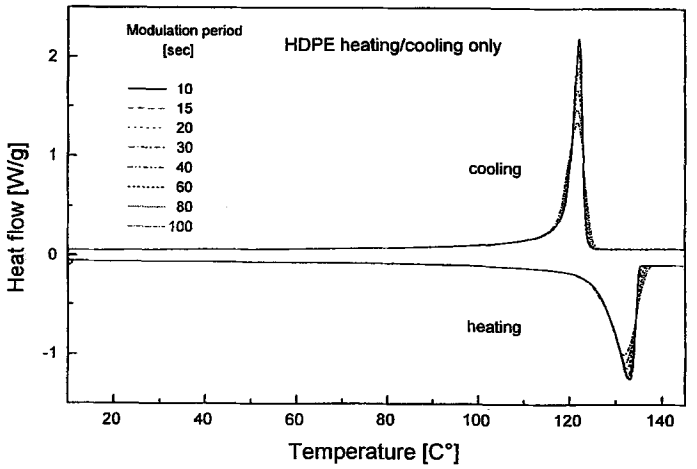

Fig. 8 Total heat flow of HDPE recorded with different modulation periods using tangential amplitude

The mean values of the error in the heat flow are about 5% and are summarised in Table 3. These values also include the error in the absolute values of the baseline shift which does not influence the calculated transition enthalpy of the crystals. The shape of the melting peaks slightly depended on the modulation frequency due to material properties. Therefore the data which form these artificial peaks were excluded from the calculation. The error (E_2 from Eq. (5)) is very high (8–60%) when the melting peak was also included in the calculation.

Figure 9 shows the heat capacities transformed to the zero frequency modulation using K=6.3 s as constant in Eq. (7). Excellent reproduction of the curves was observed at temperatures outside the melting and the crystallisation ranges. The melting process seems to be frequency dependent and because of the above mentioned artefact in the crystallisation process, the heat capacities recorded by p=10 s modulation period do not fit the general scheme.

The error differences in the heat capacities of the individual runs compared to the mean values have been calculated for the range preceding and succeeding the melting peak. The data are also summarised in Table 3.

Both the total heat flow and the heat capacities of the melting range depend on the modulation frequency. As the heat capacities of the melting range are highly dependent on the frequency, consequently the reversible heat flows are too, the kinetic heat flow must also be dependent on it. The data illustrating this is not included and will be discussed elsewhere [9]. The frequency dependence on the heat capacities and the reproducibility of the heat capacity functions by recalculation for other materials will be given here in order to show the reliability of this analysis.

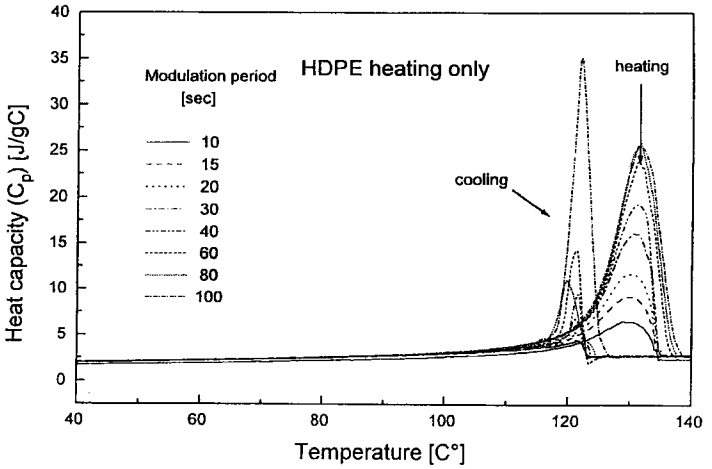

Fig. 9 Recalculated heat capacities of HDPE using Eq. (7) with K=6.3 s. Tangential amplitude

The experiments and the calculations have been repeated using deep and medium modulation amplitude for HDPE and tangential and deep modulation for the other polymers (LDPE, PP and PET). The results obtained showed similar relationships presented above. The corresponding data can be found in Table 3. The Figures are not shown in this paper but they are available on request. The constant used in Eq. (7) varied from 6.08 to 6.44 with a fairly good SD of 0.05 to 0.14. The recalculation of the heat capacities to the zero frequency value produce errors of 2 to 3%. The reproducibility of the total heat flow contained higher errors. These were greatest in the deep modulation experiment of PP and in the case of PET.

The reproducibility of the DSC curves of PET was generally lower than that of the other polymers. We used different samples for each experiments here, so the error also includes the error derived from different sample size and geometry. The DSCcurves recorded two different modulation period were different from those of the others. The weight of these samples were less than 6 mg, the weight of the others were above 10 mg.

The dependence of the heat capacities on the flow rate of purge gas

Heat capacities of the PP from 40 to 110°C have been measured in different runs where values of the flow rate of helium were varied. Each run consisted of four cycles from 40 to 100°C. Each part of the cycle was run with different modulation periods (p=10, 15,...100 s) with a deep modulation amplitude. The heat capacities at 50, 60, 70, 80 and 90°C have been read and represented as the function of the modulation periods. Two of the data series obtained by a zero flow rate and by that of 100 [ml min^{-1}] are represented on Figs 10 and 11. A third order least

Table 3 Data on reproducibility measured for different materials at different conditions

Material and method	*K*/min	STD/min	Errors in heat capacities				Errors in total heat flow			
			E_1/%		E_2/%		E_1/%		E_2/%	
			heat	cool	heat	cool	heat	cool	heat	cool
HDPE tangential	6.22	0.061	5.46	2.08	5.60	2.99	5.91	2.18	6.76	2.28
HDPE deep	6.21	0.057	3.29	0.82	3.40	2.58	4.73	4.09	4.89	4.29
HDPE 1K min^{-1}	6.34	0.051	3.90	1.09	4.09	2.08	4.86	1.58	5.01	1.59
LDPE tangential	6.40	0.107	2.07	2.85	2.54	3.36	4.60	1.94	4.78	1.95
LDPE deep	6.58	0.090	1.92	2.73	1.98	2.82	3.16	3.99	3.04	4.18
PP tangential*	6.44	0.101	1.92	1.68	2.34	2.04	1.87	3.71	1.81	3.80
PP deep$^{\$}$	6.63	0.090	2.30	2.30	2.38	2.38	5.13	6.93	5.55	6.94
PP 1st run	6.10	0.138	–	–	–	–	–	–	–	–
PET 2nd run$^{\#}$	6.08	0.137	3.08	2.78	3.87	2.76	6.22	7.00	7.72	6.99

*without data of p=10 s with 10 sec: 5.92±0.085 [min]
$^{\$}$without data of p=10 s with 10 sec: 5.99±0.109 [min]
$^{\#}$without data of p=10 s.

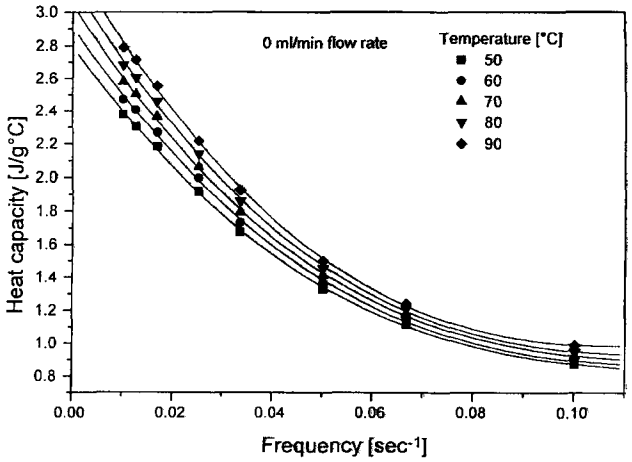

Fig. 10 The dependence of the heat capacities of PP on the modulation frequency using deep modulation amplitude. Flow rate of helium is 0 ml min^{-1}

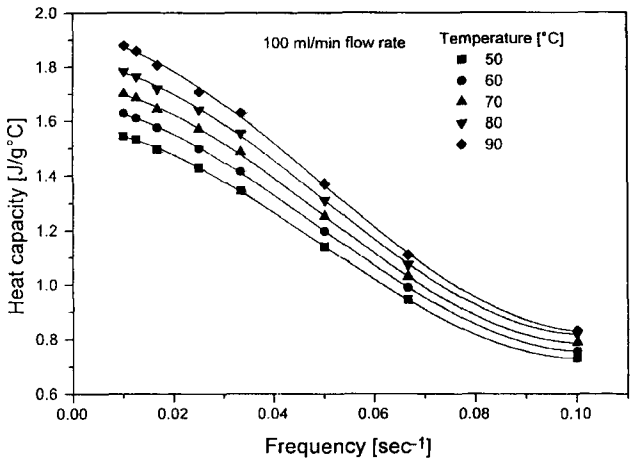

Fig. 11 The dependence of the heat capacities of PP on the modulation frequency using deep modulation amplitude. Flow rate of helium is 100 ml min^{-1}

square fit has been used to get the zero frequency heat capacities for each of the runs.

The extrapolated zero frequency heat capacities are represented as the function of the flow rate of helium in Fig. 12. Without purge gas the heat capacities are very high. Starting from 10 ml min^{-1} a second order curve has been fitted to the data. The parameters have been normalised to those measured at 100 ml min^{-1} flow rate and are given in Eq. (8):

$$K(He) = K^{\circ}(1.298 - 0.004424He + 1.438 \cdot 10^{-5}He^2) \quad (8)$$

where He is the flow rate of the helium in ml min^{-1} units, K° is the cell constant at our calibrating flow rate of 100 ml min^{-1}. The SD of the fitted parameters in Eq. (8) is 2%.

Up to 80 ml min^{-1} the value of the cell constant changes rapidly. From here on the dependency is smaller. This latter range of flow rate of helium is the most suitable to be used for accurate and reproducible measurements.

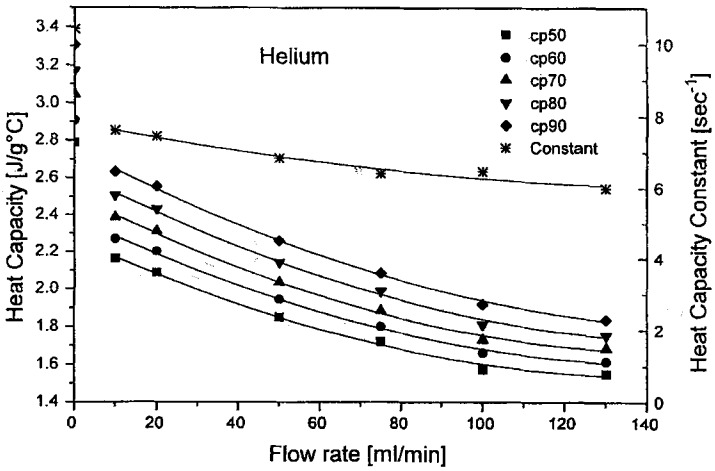

Fig. 12 The dependence of the heat capacities of PP reduced to the zero modulation frequency and of the heat capacity constant on the flow rate of helium

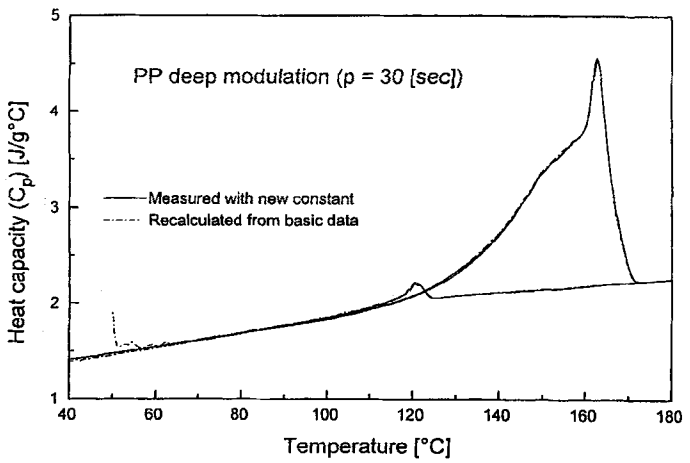

Fig. 13 Comparison of the calculated heat capacities of PP to those measured using the frequency dependent C_p constant

The constant K used in Eq. (7) depends also on the flow rate as can be seen in Fig. 12. Above 60 ml min^{-1} the constant does not change significantly. Eq. (9) describes this dependence:

$$C_p(He) = C_p^o(7.838-0.02244He+0.6819\cdot10^{-4}He^2) \quad (9)$$

where C_p^o is the zero frequency heat capacity measured at 100 ml min^{-1} flow rate.

Figure 13 shows two independent runs for PP using p=40 s as modulation frequency. The Figure contains two curves: one was recorded during the frequency studies, the other was recorded independently with the new calculated constant. The flow rate of helium was 100 ml min^{-1}. Excellent reproducibility of the heat capacities as well as the heat flows (not shown) was observed.

Conclusions

From the calibration data we can conclude that reproducible and correct results can be obtained by the TA Instrument Modulated DSC 2920. The baseline is fairly independent of the instrument parameters. The total heat flow and the heat capacities depend on several parameters, therefore these parameters should be kept constant during the runs. If the conditions (modulation periods and purging gas flow rate) differ from the values used for the calibration, the data may – and should – be recalculated to the "standard" conditions. The amplitude of the modulation has no influence on the data except for the response of the polymers in the melting range which depends both on the modulation period and on the amplitude. This phenomenon is a material property which will be discussed in a separate paper [9].

The same equation described the variation of the heat capacities with all of the tested materials. The constant obtained from the least square fit of the data varied from 6.10 to 6.8 s (Table 3). The mean value is 6.3±0.3 s, and this fixed value was used to calculate the heat capacities.

We recommend the use of a relatively large (80–110 ml min^{-1}) flow rate of helium together with a relatively small heating/cooling rate (1–2 K min^{-1}) and a moderately small modulation period (p=30–40 s) for the studies of the thermal behaviour of the polymers. The deep modulation reduces the reversible heat flow at the melting range but it is preferred to the tangential modulation, because the noise of the records is lower. It is not recommended to use the p=10 s modulation period. Very long modulation periods are not advised as they can produce artificial peaks particularly at the crystallisation of the polymers although the noise is less with greater periods.

References

1 M. Reading, D. Elliott and V. L. Hill, J. Thermal Anal., 40 (1993) 949.
2 P. S. Gill, S. R. Sauerbraun and M. Reading, J. Thermal Anal., 40 (1993) 931.

3 Manual for MDSC, TA Instrument Inc. (1994).
4 A. Boller, Y. Jin and B. Wunderlich, J. Thermal Anal., 42 (1994) 307.
5 B. Wunderlich et al., Modulated Differential Scanning Calorimetry; Summary of Eq.s and Derivations Needed for the Understanding of MDSC, For internal use of the ATHAS Group, November 8, 1995.
6 T. Ozawa and K. Kanari, Preprints of The Fourtli Asian Thermophysical Properties Conference, Tokyo 1995, p. 263.
7 T. Ozawa and K. Kanari, Thermochim. Acta, 253 (1995) 183.
8 Perkin Elmer Co, When is a DSC not a DSC and How Does it Work Anyway, in Thermal Analysis Newsletter, No. 9.
9 F. Cser, F. Rasoul and E. Kosior, to be published.
10 Handbook of Chemistry and Physics, Ed. D. R. Lide, 76th ed. 1995–96, p. 12.171.